Marine Fisheries:
Journal of Marine Fisheries Technology and Management
Vol. 17, No. 1, February 2026
Page: 13-24
https://doi.org/10.29244/1skscw50

P-ISSN 2087-4235
E-ISSN 2541-1659

Analysis of Ship Motion Response to Hull Line Redesign of The Manado Prototyped Small Purse Seiner

Heffry Veibert Dien[1]*, Revols Dolfi Christian Pamikiran[1], Lusia Manu[1], Nani Ingrid Jacquline Undap[2], Fransisco Philep Theodorus Pangalila[1], Lefrand Manoppo[1]

[1] *Fishing Technology, Faculty of Fisheries and Marine Sciences, Sam Ratulangi University, Manado 95115, North Sulawesi, Indonesia. heffryvdien@unsrat.ac.id; rdolfishp@unsrat.ac.id; manulusia@unsrat.ac.id; fransisco_pangalila@unsrat.ac.id; lefrandmanoppo@unsrat.ac.id;*
[2] *Research Center for Biota Systems, Research Organization for Life Sciences and Environment. National Research and Innovation Agency. Jl. Raya Jakarta-Bogor KM 46, Cibinong, Bogor, Jawa Barat 16911. nani015@brin.go.id*

**Correspondence: heffryvdien@unsrat.ac.id*

Received: September 17th, 2025; Revised: Desember 12th, 2025; Accepted: Januari 13th, 2026

ABSTRACT

Hull line determines the ship motions in adapting to the ocean conditions, and therefore, ships require a flexibly appropriate hull line to have a highly safe sailing trip. This study aims to determine influence of small purse-seiner hull line redesign on the ship's motion, namely rolling, heaving, and pitching which can be observed as a Response Amplitude Operator (RAO) due to the sea conditions. The hull lines were redesigned by manipulating the ship's breadth (B) and depth (D) based on the Manado prototype, resulting in three new hull forms (ships B, C, D) and one prototype control (ship A). Data input and simulation used the Maxsurf Modeler Advanced and Maxsurf Motions Advanced applications to analyze motion responses at different wave angles (head sea 180°, bow quartering sea 135°, and beam sea 90°) under average load and service speed conditions. The findings demonstrated that each ship had a unique RAO for heave, roll, and pitch motion. In heave and pitch motion, ship D had a best RAO, but in roll motion, ship C had the best RAO. The rolling and pitching motions of all ships have met the minimum standard of the general operability limiting criteria for ships at all conditions, while the rolling motion at the wave coming of 90° was met at the slight and moderate conditions.

Keywords: *Heaving motion, North Sulawesi-Indonesia, pitching motion, rolling motion, ship motion*

INTRODUCTION

Indonesian fishing boats with a size below 25 meters are generally still planned and made traditionally (Mulyatno *et al*. 2019). Traditional fishermen have long used a fleet of wooden boats and even there are recently still many fishermen using it due to its cheaper manufacturing procedure than that of steel boats (Chrismianto *et al*. 2020; Liu *et al*. 2019). A purse seiner is one of the fishing vessels with distinctive shapes based on the locality where the ship is made. Although the shape and size are different with the locality, they are all intended for the purpose of ship activities where the ship's motion response capability is absolutely needed to support the secure fishing operation of the purse-seiner in the ocean. In addition to the ship shape coefficient itself, the principal dimensions such as the ship's length (L), breadth (B), and depth (D) and their comparison will also determine and reflect the ship's performance on the water, including stability, resistance, load ability, and motion (Pamikiran *et al*. 2017; Pamikiran *et al*. 2020; Prabowo *et al*. 2022;

Saifullah *et al*. 2024; Dien *et al*. 2025). There are six known ship motions (rotational motion and linear motion), namely yaw, pitch, roll, heave, sway, and surge (Alqurashi *et al*. 2022; Darmawan *et al*. 2022) (Fig. 1).

A ship's Response Amplitude Operator (RAO) is the ship's ability to respond to sea conditions in three forms of motion: heaving, rolling, and pitching (Fajar *et al*. 2017; Ghassemi *et al*. 2015). Moreover, the relationship between the amplitude of an ocean wave and the amplitude of a ship's response is represented by the Response Amplitude Operator (RAO), also referred to as the Transfer Function (Rahmaji *et al*. 2022). Due to waves striking the hull structure within a specific frequency band, RAO is a transfer function. RAO is a transfer function due to waves hitting the hull structure in a certain frequency range. These three movements (rolling, heaving, and pitching) are oscillatory movements due to the effect of the damping force when the ship changes from its equilibrium position. The ship does not return to its initial equilibrium position while surging, swaying. or yawing, unless the force or moment causing the change acts from the opposite direction.

In the phenomenon of ship movement, the forward or backward movement, if the ship moves at a constant speed, then the wave will appear to be faster than the actual frequency of the sea waves it faces. The observed frequency is called an encounter frequency. Like waves, encounter frequency has an encounter period (Te), the time a ship takes to move from one wave peak to another. The encounter period is a function of the wave period (T), the ship's velocity (V), and the angle of encounter (μ). RAO analysis is used to estimate the maximum transfer function for every movement of the ship (heave, roll, and pitch) at the encounter frequency and at the frequency of the incoming waves. This implies that by determining the natural frequency of the waves and the ship's motion, it is possible to identify a potential resonance between the wave frequency and the ship's mo-tion frequency. This resonance can be detected through the maximum transfer function observed in the ship's motion.

The Operator's Amplitude Response (RAO) is the term used to describe the motion of a structure in regular waves that represents the relationship between the amplitude of the structure's movement and the amplitude of the wave (Ghadimi *et al*. 2020; Heriyanty *et al*. 2019; Kusumah *et al*. 2018). Information on the maximum transfer function at each ship's movement can indicate the quality of the ship design, in which a good design is indicated by a small maximum transfer function value. There are many ways to find out the RAO, ranging from the tests using models in the towing tanks to numerical and analytical approaches using either manual or certain programs. It is important to understand how the ship will react or maneuver when waves strike the ship's structure (Suzuki *et al*. 2023). RAO is used to forecast ship movement reactions, including heave, roll, and pitch, using numerical models (Ibinabo & Tamunodukobipi 2019; Virliani *et al*. 2017). Purse seine fisheries in North Sulawesi Province are located in several regions, such as Bitung, Molibagu, Belang, and Manado, but the ship shapes are different with regions. Previous findings Pamikiran *et al*. (2017) indicate that the purse seiner of Manado has the best technical ability among the others. Manado purse seiners is well known to have a good technical capability of movement response (rolling, heaving, and pitching). However, since they are traditionally made, the stability performance could still be increased through hull shape modifications. The hull redesign can yield better movement response which also impacts on the safety and the comfort of the ship crews in various ocean conditions. Therefore, this design is adopted as a prototype to make a new design to be able to increase its technical ability, particularly the ship motion. The study on the Response Amplitude Operator (RAO) of the redesigned purse seiner is important to ensure the ship safety in different ocean conditions of the fishing operations. Therefore, it focused on determining the influence of small purse-seiner hull line redesign on the ship's motion response, namely rolling, heaving, and pitching which can be observed as a Response Amplitude Operator (RAO) due to the sea conditions.

https://doi.org/10.29244/1skscw50

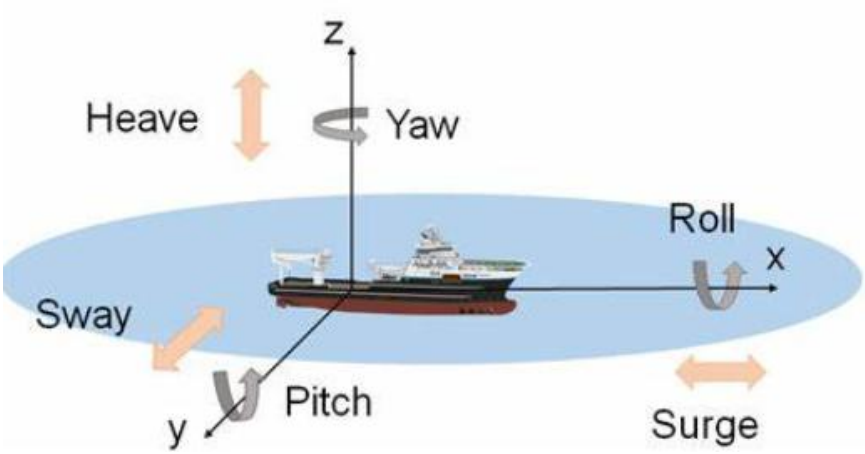

Figure 1 Six degrees ilustration of freedom for the ship movement

METHODS

1. Data Sources

The study was accomplished from November 2019 to April 2021 covering field data collection, measurements, and analysis. The redesigned ship model was adopted from the original ship shape of Manado that has the best resistance and stability among the purse seiners in North Sulawesi Province. The hull line measurement of the prototype ship's hull line from Manado city was utilized as the basis of the data (Pamikiran *et al*. 2017). The hull line of the Manado prototype ship was redesigned by manipulating the ship's width (B) and depth (D). Therefore, the hull line structure design changed in a three dimensional direction. The ratio between the principal dimensions of Length (L), Width (B), and Depth (D) were set for the purse seiner as L/B = 3.10 - 4.30, B/D = 2.10 - 5.00, and L/D = 9.50 - 11.00, respectively (Fyson 1985). The dimension ratio midpoints (L/B = 3.7. B/D = 3.5, and L/D = 10.25) were adopted to obtain 3 new hull line forms, with the prototype ship as control and coded as A (prototype), B, C, and D. The hull line drawings and the main sizes of the ships are presented in Figure 1, 2, 3, and 4 (Pamikiran *et al*. 2020). The use of 3 hull line designs is based on Pamikiran *et al*. (2017) who to examine the velocity and stability at 3 different locations (Bitung, Manado, and Molibagu), this process led to the selection of the vessel with the best stability (Manado prototype) which then became the subject of a stability analysis for its redesigned hull lines (Pamikiran *et al*. 2020). Then, currently, research is being continued on the ship's motion response, namely rolling, heaving, and pitching, which can be observed as Response Amplitude Operators (RAO) due to sea conditions during fishing operations.

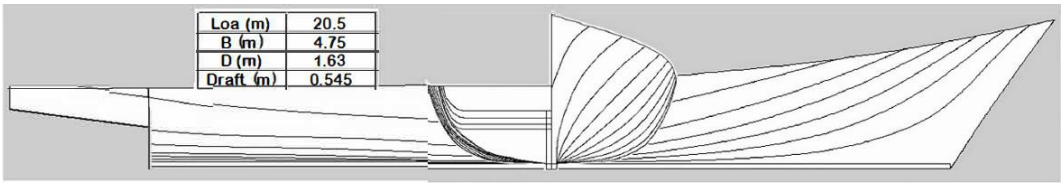

Figure 2 Hull line and principal dimension of ship A (prototype)

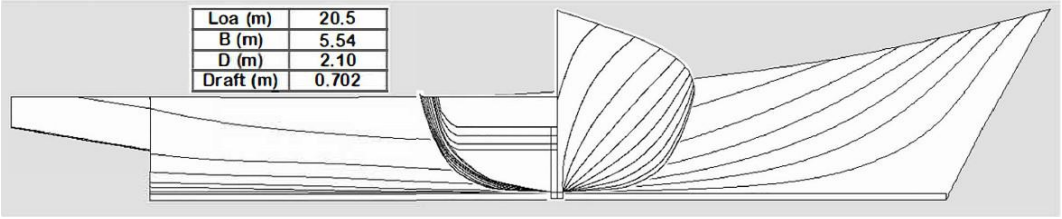

Figure 3 Hull line and principal dimension of ship B (1st redesigned)

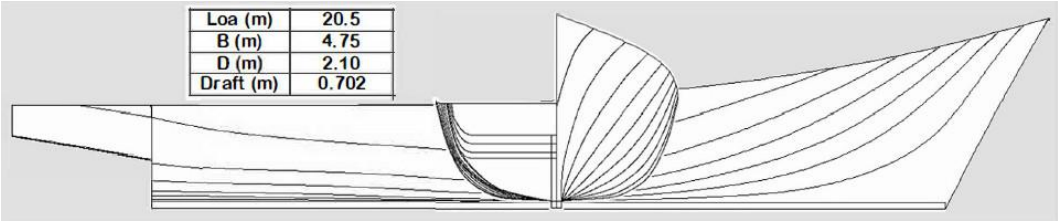

Figure 4 Hull line and principal dimension of ship C (2nd redesigned)

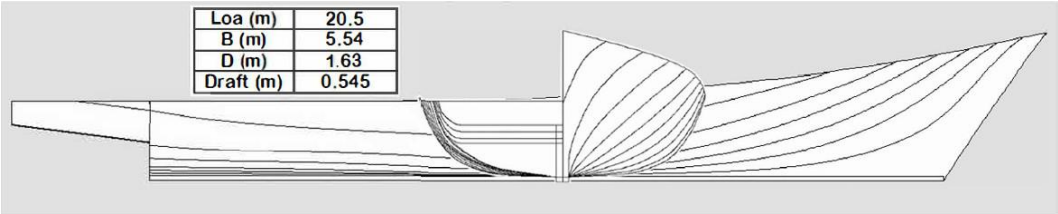

Figure 5 Hull line and principal dimension of ship D (3rd redesigned)

The Maxsurf Modeler Advanced application was used to input the image data of the ship's hull line, as this study utilized virtual simulations. The image data of the hull line and the main dimension were formatted appropriately (msd) for RAO analysis using the Maxsurf Motions Advanced application. Wave arrival data, such as beam sea (90°), bow quartering sea (135°), head sea (180°), and mean load and ship's speed, were also involved.

The research methodology in this study was conducted computationally through three key stages: first, modeling the hull lines of ships A, B, C, and D into 3D models using Maxsurf Modeler Advanced; second, simulating ship motion responses (heave, roll, pitch) to varying wave directions (90°, 135°, 180°) under operational load and speed conditions using Maxsurf Motions Advanced to generate Response Amplitude Operator (RAO) curves; and third, analyzing maximum RAO values and simulating actual ship motions using the JONSWAP wave spectrum to evaluate performance and compliance with operability criteria across different sea conditions.

2. Data Analysis

For the purposes of ship motion analysis, hull line data were inputted together with other supporting data into the Maxsurf Motions Advanced application. The formulation of several parameters related to the ship's motion was referred to Bhattacharya (1978) as follows:

$$T_e = \frac{L_w}{V_w - V\,\boldsymbol{Cos}\,\mu} \quad \text{.....(1)}$$

$$\omega_e = \omega_w\left(1 - \frac{V}{V_w} Cos\,\mu\right) \quad \text{.....(2)}$$

Where:
Te = encountering period(s)
ωe = encountering frequency (rad/sec)
ωw = wave frequency (rad/sec)
Vw = wave speed (m/s)
Lw = wave length (m)
V = ship speed (knots), and
μ = angle of incidence wave

The Response Amplitude Operator (RAO) serves as a transfer function that helps transfer external loads, such as waves, into responses for a structure (Bhattacharya, 1978). RAO is expressed in mathematical form as ζ-response/ζ-wave, where the amplitude of the response can be motion, tension, or vibration.

$$RAO = \frac{X_p\,(\omega)}{\eta\,(\omega)} \quad \text{.....(3)}$$

Where:
Xp (ω) = amplitude of ship movement
η (ω) = amplitude of the wave incidence

Heaving movement is the vertical movement of the ship. It was analysed as follows:

$$a\ddot{z} + b\dot{z} + cz = F0\ Cos\ \omega et \quad \text{.....(4)}$$

Where:
az̈ = inertial force Fa
bż = damping force Fb
cz = restoring force Fc
$F0\ Cos\ \omega et$ = exciting force

The rolling movement is the movement of the ship around the axis when a longitudinal

rolling occurs alternately towards the right and the left side. The rolling movement analysis used the following formula:

$$a\frac{d^2\emptyset}{dt} + a\frac{d\emptyset}{dt} + c\emptyset = Mo.Cos\ \omega_e t \text{.....(5)}$$

Where:

a (d^2ø)/dt = inertial moment

a (dø)/dt = damping moment

$c\emptyset =$ restoring moment

$Mo\ cos\ \omega e$t. = exciting moment

The pitching movement is the motion of the ship that causes the ship trim either bow or stern part occur alternately. This movement was analysed as follows:

$$d\ddot{\theta} + e\theta + h\theta = Mo\ Cos\ \omega et \text{.....(6)}$$

Where:

$d\frac{d^2x\,\theta}{dt^2}$ = inertial moment

$e\frac{d\theta}{dt}$ = damping moment

He = restoring moment

$M_o\ Cos\ \omega_e t$ = exciting moment

RESULTS

The analysis of ship motion, i.e. heave, roll, and pitch, was applied to four different ships by considering the three-angle approach in beam sea (90°), bow quartering sea (135°), and head sea wave (180°) conditions at average load conditions and the ship's operational speed. The RAO curve as an effect of the various states applied to the four vessels of the object, and the encounter frequency, wave frequency, and transfer function values of each heave, roll, and pitch ship motion are presented in figure 6-13. The RAO for the maximum transfer function on the ship motion range is presented in Table 1.

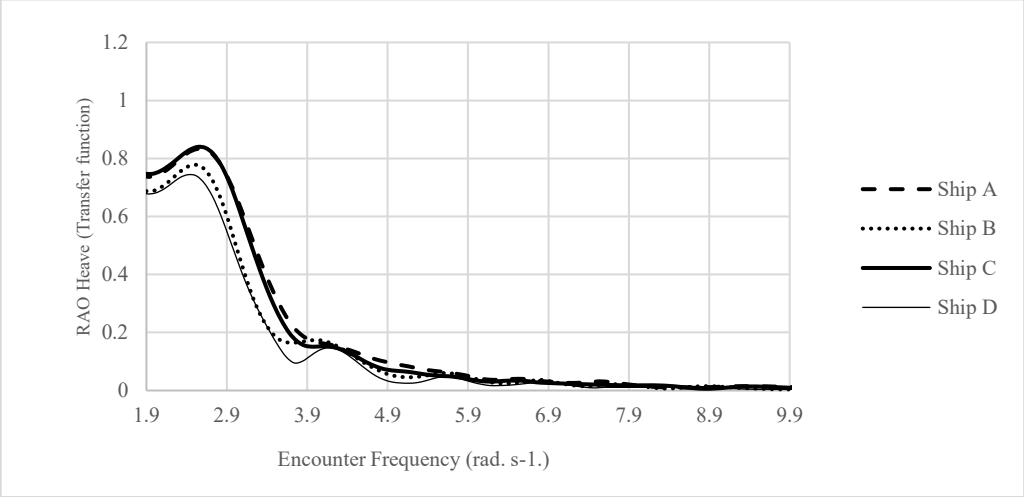

Figure 6 RAO heave of the ship prototype (Ship A) and the ship redesigned (Ship B, C and D) at 8.56 knots and the encounter angle of 90º

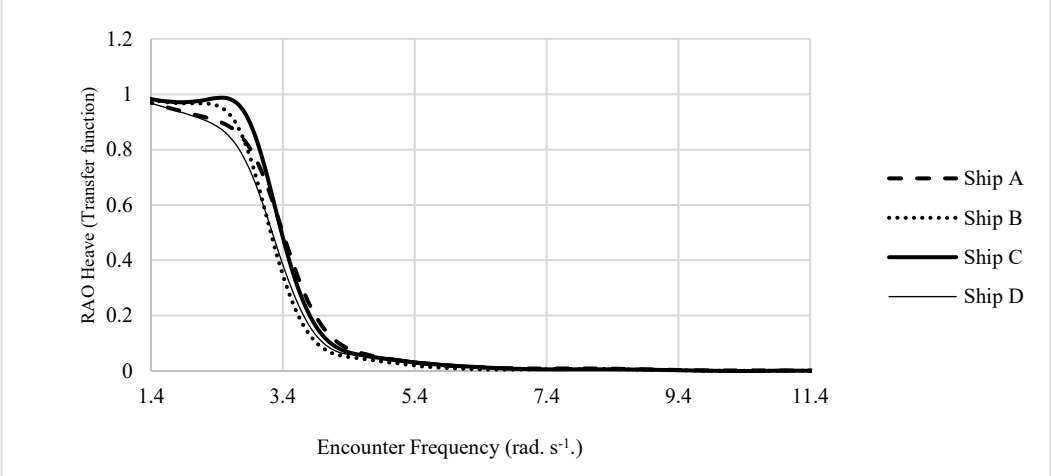

Figure 7 RAO heave of the ship prototype (Ship A) and the ship redesigned (Ship B, C and D) at 8.56 knots and the encounter angle of 135º

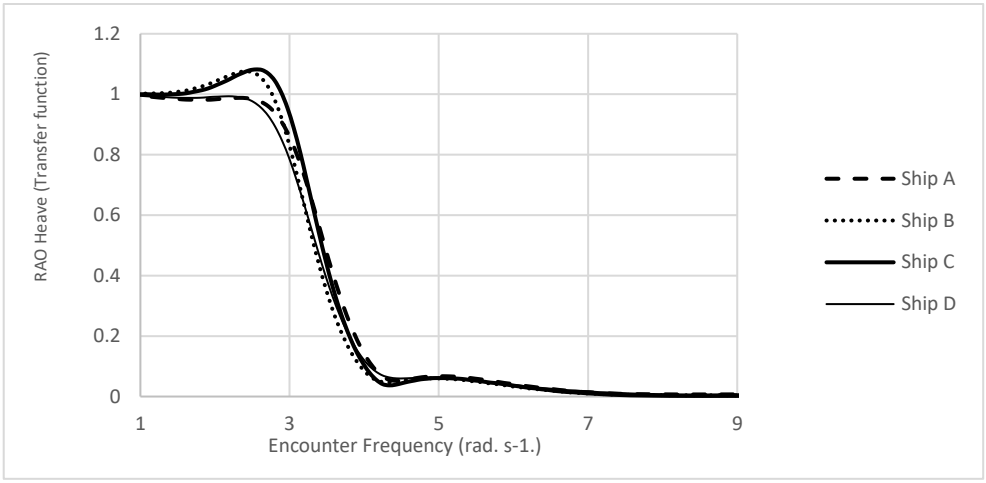

Figure 8 RAO heave of the ship prototype (Ship A) and the ship redesigned (Ship B, C and D) at a speed of 8.56 knots and the encounter angle of 180º.

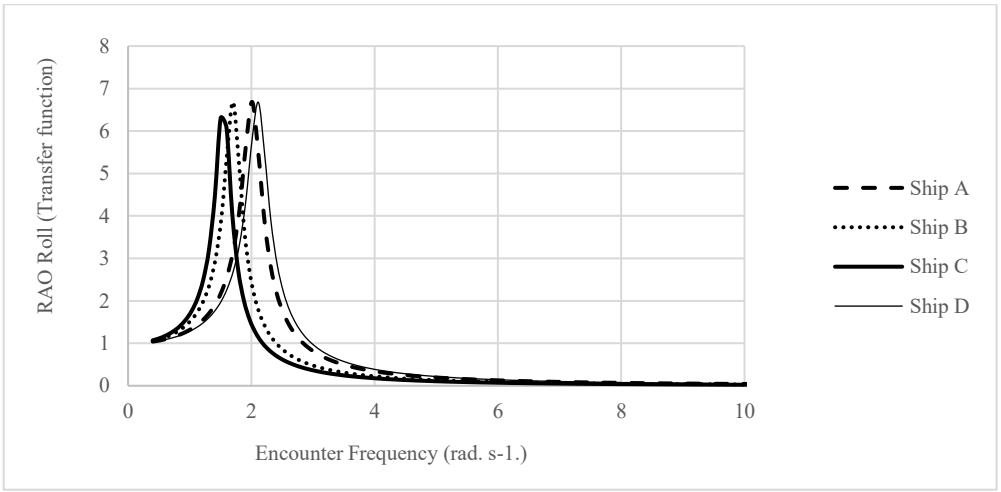

Figure 9 RAO roll of the ship prototype (Ship A) and the ship redesigned (Ship B, C and D) at 8.56 knots and the encounter angle of 90º

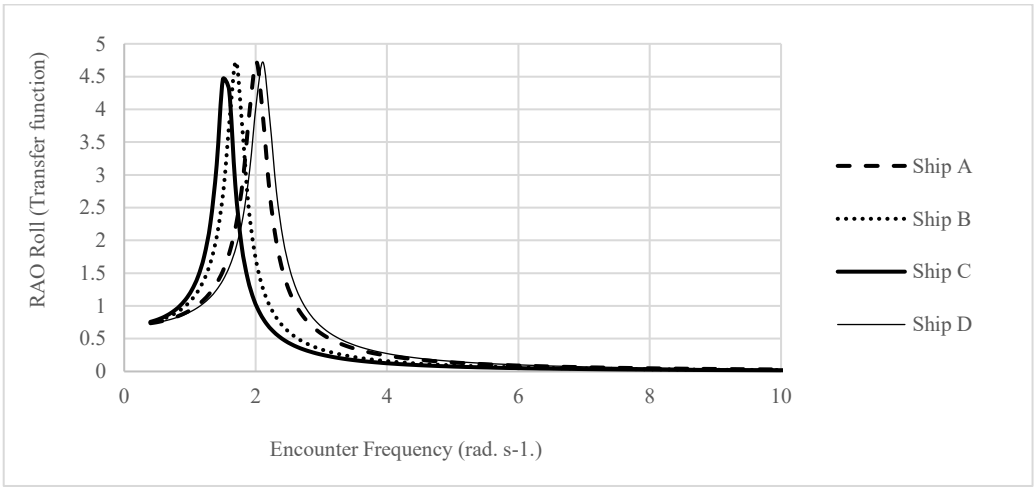

Figure 10 RAO roll of the ship prototype (Ship A) and the ship redesigned (Ship B, C and D) at 8.56 knots and the encounter angle of 135º

https://doi.org/10.29244/1skscw50

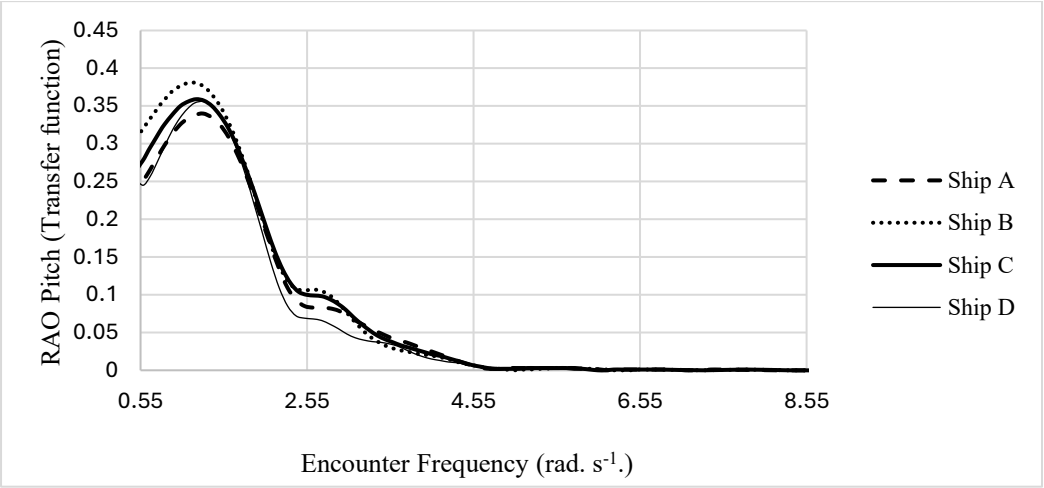

Figure 11 RAO pitch of the ship prototype (Ship A) and the ship redesigned (Ship B, C and D) at 8.56 knots and the encounter angle of 90º.

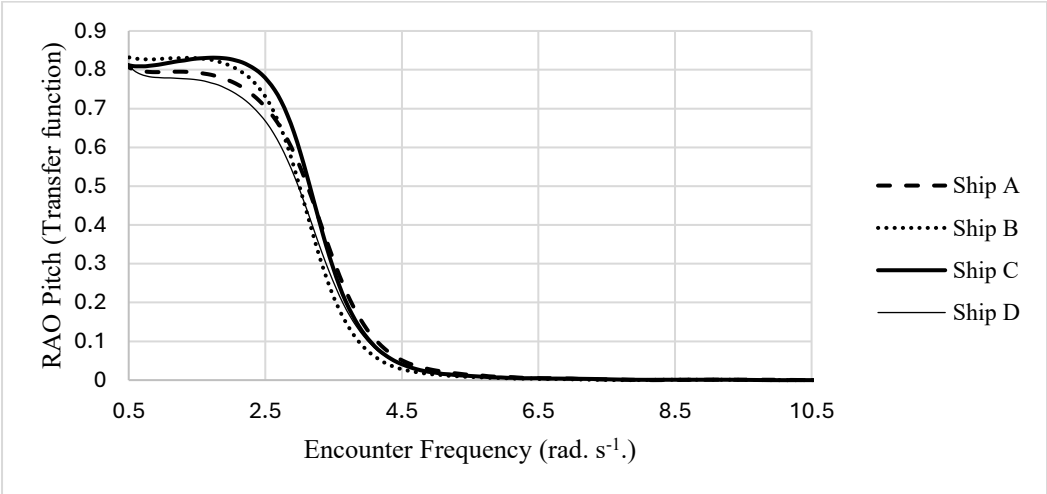

Figure 12 RAO pitch of the ship prototype (Ship A) and the ship redesigned (Ship B, C and D) at 8.56 knots and the encounter angle of 135º

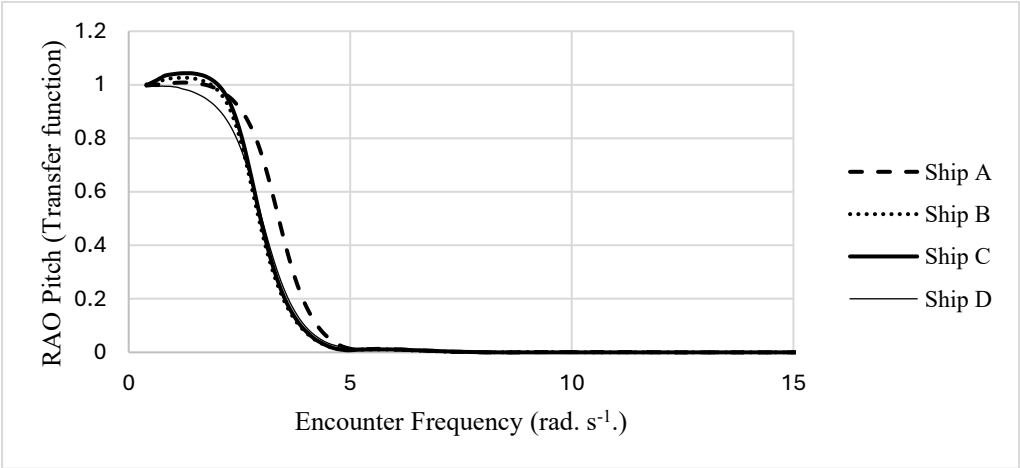

Figure 13 RAO pitch of the ship prototype (Ship A) and the ship redesigned (Ship B, C and D) at 8.56 knots and the encounter angle of 180º

Table 1 RAO values of ships based on the encounter angle on the prototype ship (A) and the three redesigned ships (B, C, and D)

Ship	Encounter angle (degree)	Rerponse Amplitudo Operator (RAO)	Encounter frequency (rad. s-1)	Transfer function (m or degree)
A	90	Heave	2.927	0.725
B	90	Heave	2.907	0.596
C	90	Heave	2.921	0.724
D	90	Heave	2.927	0.528
A	135	Heave	2.419	0.902
B	135	Heave	2.443	0.955
C	135	Heave	2.448	0.987
D	135	Heave	2.419	0.881
A	180	Heave	2.519	0.983
B	180	Heave	2.461	1.075
C	180	Heave	2.546	1.082
D	180	Heave	2.231	0.993
A	90	Roll	2.013	6.684
B	90	Roll	1.702	6.685
C	90	Roll	1.502	6.303
D	90	Roll	2.114	6.675
A	135	Roll	2.013	4.727
B	135	Roll	1.702	4.727
C	135	Roll	1.502	4.457
D	135	Roll	2.114	4.720
A	180	Roll	-	-
B	180	Roll	-	-
C	180	Roll	-	-
D	180	Roll	-	-
A	90	Pitch	1.302	0.340
B	90	Pitch	1.145	0.381
C	90	Pitch	1.218	0.359
D	90	Pitch	1.302	0.356
A	135	Pitch	1.708	0.787
B	135	Pitch	1.794	0.822
C	135	Pitch	1.786	0.831
D	135	Pitch	1.708	0.766
A	180	Pitch	1.302	1.008
B	180	Pitch	1.238	1.026
C	180	Pitch	1.313	1.043
D	180	Pitch	1.302	0.981

To support the outcome above, the ship movements were analysed using Joint North Sea Wave Project (JONSWAP) application at the wave spectra for Indonesian Sea conditions, particularly Northern Sea and archipelagic conditions (Gustiarini *et al*. 2017; Mazzaretto *et al*. 2022). The wave condition categories followed the World Meteorological Organization (WMO) as presented in Table 2.

Table 3 demonstrates the lowest movements at different encounter angle and different redesign simulations that at the encounter angle of 90°, the lowest heave movement was recorded in ships B and D, 0.211 m (slight), B and D, 0.460 m (moderate), and B and D, 0.802 m (rough); the roll movements occurred only in ship C at all coming angles and sea conditions; pitch was recorded in ships A and D at different coming angles and sea conditions.

https://doi.org/10.29244/1skscw50

Table 2 Ocean condition categorized by the World Meteorological Organization (WMO)

Sea State Code	***Significant Wave Height* (m)**		***Description***
	Range	**Means**	
3	0.5 – 1.25	0.875	*Slight*
4	1.25 – 2.5	1.875	*Moderate*
5	2.5 – 4.0	3.25	*Rough*

Source: metservice.com

Table 3 Roll, heave, and pitch amplitude of prototype vessels (A) and redesigned vessels (B, C, and D) simulations result in encounter angle (90°, 135°, and 180°) for each ocean condition (slight, moderate, rough)

Encounter angle		Slight			Moderate			Rough		
		Heave (m)	Roll (deg.)	Pitch (deg,)	Heave (m)	Roll (deg.)	Pitch (deg,)	Heave (m)	Roll (deg.)	Pitch (deg,)
90º /	A	0.213	3.62	0.35	0.462	5.72	0.58	0.804	8.22	0.85
	B	0.211	3.54	0.40	0.460	5.62	0.66	0.802	8.10	0.98
	C	0.213	3.47	0.37	0.463	5.53	0.62	0.806	7.99	0.91
	D	0.211	3.64	0.35	0.460	5.74	0.58	0.802	8.25	0.86
135º /	A	0.214	2.15	0.85	0.464	3.46	1.43	0.807	5.02	2.14
	B	0.215	2.09	0.87	0.465	3.40	1.48	0.809	4.95	2.21
	C	0.216	2.03	0.89	0.466	3.33	1.50	0.810	4.88	2.24
	D	0.214	2.17	0.82	0.463	3.48	1.39	0.806	5.04	2.08
180º /	A	0.215	0	1.03	0.465	0	1.74	0.808	0	2.61
	B	0.218	0	1.04	0.469	0	1.77	0.813	0	2.64
	C	0.218	0	1.07	0.468	0	1.81	0.813	0	2.70
	D	0.215	0	0.99	0.465	0	1.70	0.808	0	2.54

DISCUSSION

The maximum heave motion at the wave angles of 90º, 135º, and 180º, occurs at an angle of 180º, and it is in accordance with the previous finding Putranto & Sulisetyono (2015); Romadhoni (2019); Harry-Ameh *et al*. (2021). The motion of RAO heave at the wave incidence angle of 90º, two small maximum transfer function value occurs on ships B (encounter frequency of 2.907 rad. s-1, with the transfer function of 0.596 m) and D (encounter frequency of 2.927 rad. s-1, with the transfer function of 0.528 m). The motion of RAO heave at the angle of arrival of wave 135º, two small maximum transfer function value occurs on ships A (encounter frequency of 2.419 rad. s-1, with the transfer function of 0.902 m) and D (encounter frequency of 2.419 rad. s-1, with the transfer function of 0.881 m). At 180º of the coming wave angle, two small maximum transfer function values occur on ship A (encounter frequency of 2.519 rad. s-1, with the transfer function of 0.983 m) and ship D (encounter frequency of 2.231 rad. s-1, with transfer function of 0.993 m).

In the three directions of the coming wave (μ), the RAO heave motion that occurs on ships A and D is smaller than ships B and C, because the height of ships B and C is greater than that of ships A and D, which can lead to an increase in the value of the ship's displacement (∆) and will ultimately affect the heave response value of these ships and the sailing comfort.

The roll motion does not occur at the wave angle of 180º because the coming wave is perpendicular to the ship. It is in accordance with that rolling movement usually occurs at the angle of arrival of waves 90º and 135º, and maximum at an angle of 90º (Göksu & Bayramoğlu 2021; Romadhoni 2016; Romadhoni 2019). At the roll angle of 90º, small maximum transfer functions occur on ships C (encounter frequency of 1.502 rad. s-1, with the transfer function of 6.303º). The roll motion at the wave arrival angle of 135º gave small maximum transfer function values on ship C (encounter frequency of 1.502 rad. s-1, with the transfer function of 4.457º).

Similar to the heave motion, the pitch motion occurs at the coming wave angle of 90º, 135º, and 180º, where the maximum value occurs at an angle of 180º as stated in the previous study (Fitriadhy & Adam 2017; Rahmaji *et al*. 2022). The pitch motion at the wave arrival angle of 90º, two small maximum transfer functions occur on ships A (encounter frequency of 1.302 rad/s, with transfer function

value of 0.340°) and D (encounter frequency of 1.302 rad. s-1, with the transfer function of 0.356°). At the wave arrival angle of 135°, the pitch motion yielded two small maximum transfer functions on ships A (encounter frequency of 1.708 rad. s-1, with the transfer function of 0.787°) and D (encounter frequency of 1.708 rad. s-1, with the transfer function of 0.766°). The pitch motion at the wave angle of 180° yielded two small maximum transfer functions on ship A (encounter frequency of 1.302 rad. s-1, with transfer function value of 1.008°) and ship D (encounter frequency of 1.302 rad. s-1, at the transfer function of 0.981°).

Ships A and D have better RAO values than those of B and C, meaning that the ship's response values to the two vessel's Heave and Pitch at the different arrival wave angles (90°, 135°, and 180°) are smaller than the other two vessels (B and C). The better RAO value of ships A and D compared to ships B and C could result from the condition of the shape and the ratio of the main dimension, especially the ship's height against the ship's width and length which contributes positively to the ship stability, both transversely and longitudinally, and ultimately contributes to the RAO value of ships A and D. For the rolling movement at the encounter angle of 90° and 135°, ship C had the smallest maximum response among the others (A, B, and D) reflecting that the ship C has a better rolling movement than ships A, B, and D at these encounter angle.

At the encounter angle of 135°, the lowest heave occurred in ships A and D at the slight condition, while at the moderate and rough conditions, the lowest heave occurred only in ship D; the lowest roll was recorded only in ship C at all sea conditions, while the lowest pitch occurred only in ship D. Moreover, at the encounter angle of 180°, the lowest heave was recorded in ship A and D in all sea conditions, except that there is no roll movement due to its perpendicular position to the roll direction; the lowest pitch was recorded in ship D at all sea conditions. Based on the simulation results, the best encounter angle of 90° for heave and pitch movements was found in ship D, and the roll in ship C; at the encounter angle of 135°, the best heave and pitch were found in ship D, while the best roll was recorded in ship C; at the angle of 180°, the best heave and pitch were found in ship D.

These findings indicated that ship D, in general, has the best performance in heave and pitch at all angles, while ship C showed the best performance only at the encounter angle of 90° and 135° for the roll movements. Both roll and pitch parameters are used to meet the general operability limiting criteria for ships (Ghassemi *et al*. 2015), 6° (Root Mean Square, RMS) for rolling and 3° (RMS) for pitching. The standard rolling and pitching have been met by all ships at various sea conditions, while at the encounter angle of 90°, the roll performance occurs only up to the moderate condition.

CONCLUSION

All ships used in the study met the standard criteria for rolling and pitching motions across all sea conditions (slight, moderate, and rough); however, rolling motion at a wave angle of 90° was only fulfilled under slight and moderate sea conditions. Ship D consistently demonstrated better RAO performance in heave and pitch motions than ships A, B, and C. This superiority can be attributed to the optimized main dimension ratios resulted from the hull redesign simulation, The ratio between the principal dimensions of Breadth-to-Depth (B/D) and Length-to-Depth (L/D) ratios, which improved its longitudinal stability and dampened vertical motion responses. Ship C had the best RAO for roll motion, benefitting from a lower centre of gravity and favourably transverse stability characteristics. The rolling motion at a wave angle of 90° was only fulfilled under slight and moderate sea conditions. These findings underscored the direct influence of principal dimension adjustments on motion response and support the adoption of dimension-driven hull redesign for enhanced seakeeping performance in small purse-seine vessels.

SUGGESTION

This finding has given useful information on the vessel's RAO. Future studies need to integrate the RAO analysis with a full stability assessment following the IMO/FAO guidelines for fishing vessels, particularly hull line design to ensure a safe and efficient sailing during the fishing operation.

ACKNOWLEDGMENTS

We extend our profound gratitude to the owner of the traditional purse-seiner for his kind permission and access to his vessel, which served as the essential prototype for this study. We are equally indebted to the ship's crew for their unwavering assistance, hard work, and cooperation during the on-site

measurements and data collection. Special appreciation is addressed to Prof. Dr. Ir. Silvester B. Pratasik for his meticulous proofreading and English editing, which greatly enhanced the clarity and quality of this paper. We also acknowledge the facilities and support provided by Sam Ratulangi University and the National Research and Innovation Agency (BRIN).

REFERENCES

Alqurashi FS, Trichili A, Saeed N, Ooi BS, Alouini MS. 2022. Maritime Communications: A Survey on Enabling Technologies, Opportunities, and Challenges. *IEEE Internet of Things Journal*. 10(4): 3525–3547. https://doi.org/10.1109/JIOT.2022.3219674

Bhattacharya R. 1978. *Dynamics of Marine Vehicles*. John Wiley & Sons.

Chrismianto D, Yudo H, Dewa NR. 2020. Modification of 30 GT Fishing Vessels Using Hull Vane NACA 2408 Type for Reducing Ship Resistance. *International Journal of Advanced Research in Engineering and Technology*. 11(4): 57–62.

Darmawan AB, Darma YYE, Rulianto J. 2022. Analysis The Effect of Outrigger (Cadik) Variations on Motion Response of Fishing Boat Using CFD Method. *IOP Conference Series: Earth and Environmental Science*. 1081(1): 1–15. https://doi.org/10.1088/1755-1315/1081/1/012010

Dien HV, Pangalila FPT, Modaso VOJ, Undap NIJ, Pamikiran RDCh. 2025. Study on the Stability of Purse Seiners in Manado. *International Journal of Agriculture and Biological Sciences.* 9(1)*:* 1-7. https://doi.org/10.5281/zenodo

Fajar AH, Chrismianto D, Hadi ES. 2017. Studi Analisa Slamming & Deck Wetness Akibat Gerakan Heaving – Pitching Coupling & Gerakan Non-Linier Rolling (Studi Kasus Kapal MT. Pandan). *Jurnal Teknik Perkapalan*. 5(4): 677–687. http://ejournal3.undip.ac.id/index.php/naval

Fitriadhy A, Adam NA. 2017. Heave and Pitch Motions Performance of a Monotricat Ship in Head-Seas. *International Journal of Automotive and Mechanical Engineering*. 14(2): 4243–4258. https://doi.org/10.15282/ijame.14.2.2017.10.0339

Fyson J. 1985. *Design of Small Fishing Vessel*. Fishing News Books Ltd.

Ghadimi P, Pourmostafa M, Najafi S. 2020. Investigating the Response Amplitude Operator of a Heaving Pontoon under the Influence of a Submerged Trapezoidal Breakwater. *Advances in Civil Engineering*. *2020*: 1–12. https://doi.org/10.1155/2020/8813096

Göksu B, Bayramoğlu K. 2021. Control of Ship Roll and Yaw Angles During Turning Motion. *Marine Science and Technology Bulletin*. 10(4): 340–349. https://doi.org/10.33714/masteb.930338

Ghassemi H, Majdfar S, Gill V. 2015. Calculations of the Heave and Pitch RAO's for Three Different Ship's Hull Forms. *Journal of Ocean, Mechanical and Aerospace-Science and Engineering*. *22*: 1-8.

Gustiarini ED, Arswendo B, Hadi S. 2017. Performance Analysis of the Traditional Fishing Vessel KMN. Rukun Arta Santosa 7 Due to Operational Area Relocation and Fishing Gear Replacement. *Jurnal Teknik Perkapalan*. 5(3): 530–539. http://ejournal3.undip.ac.id/index.php/naval

Harry-Ameh Orji CU, Dick IF. 2021. Effect of Coupled Heave-Pitch Motion on a Vessel Moving in Regular Water Ways. *International Journal of Advances in Engineering and Management (IJAEM)*. 3(11): 518–530. https://doi.org/10.35629/5252-0311518530

Heriyanty E, Hadi ES, Kiryanto K. 2019. Seakeeping Analysis of a Hexagonal Prism-Shaped Pontoon in Regular Waves Using Computational Fluid Dynamics (CFD) Simulation. *Jurnal Teknik Perkapalan*. 7(4): 548–556. https://ejournal3.undip.ac.id/index.php/naval

Ibinabo I, Tamunodukobipi DT. 2019. Determination of the Response Amplitude Operator(s) of an FPSO. *Engineering*. 11(09): 541–556. https://doi.org/10.4236/eng.2019.119038

Kusumah YW, Sulisetyono A, Putranto T. 2018. Analysis of the Influence of Ship

Motion on Added Wave Resistance: A Case Study of a Corvette Vessel. *Jurnal Teknik ITS*. 7(1): G105–G110. https://doi.org/10.12962/j23373539.v7i1.29670

Liu W, Demirel YK, Djatmiko EB, Nugroho S, Tezdogan T, Kurt RE, Supomo H, Baihaqi I, Yuan Z, Incecik A. 2019. Bilge Keel Design for the Traditional Fishing Boats of Indonesia's East Java. *International Journal of Naval Architecture and Ocean Engineering*. 11(1): 380–395. https://doi.org/10.1016/j.ijnaoe.2018.07.004

Mazzaretto OM, Menéndez M, Lobeto H. 2022. A Global Evaluation of the JONSWAP Spectra Suitability on Coastal Areas. *Ocean Engineering*. 266: 1–15. https://doi.org/10.1016/j.oceaneng.2022.112756

Mulyatno IP, Kirianto Chrismianto D. 2019. Investigation of Stability Criteria of Batang Type Traditional Fishing Boat Under 25 M for Safety at Sea. *International Journal of Mechanical Engineering and Technology (IJMET)*. 10(2): 1031–1035.

Pamikiran RDC, Kaparang FE, Dien HV. 2017. Study of Speed and Stability in Some form of Small Purse-Seiner in North Sulawesi. *Jurnal Ilmu dan Teknologi Perikanan Tangkap*. 2(5): 165–170. https://doi.org/10.35800/jitpt.2.5.2017.14746.

Pamikiran RDC, Masengi KWA, Kaparang FE, Dien HV, Pratasik SB. 2020. Stability of Redesigned Hull Line of Manado Prototype Purse Seine Vessel. *International Journal of Scientific & Technology Research*. 9(12): 159–162.

Prabowo AR, Muttaqie T, Martono E, Tuswan T, Bae DM. 2022. Effect of Hull Design Variations on the Resistance Profile and Wave Pattern: A Case Study of the Patrol Boat Vessel. *Journal of Engineering Science and Technology*. 17(1): 106–126.

Putranto T, Sulisetyono A. 2015. Numerical Analysis of Ship Motion and Structural Strength Due to Slamming Loads on a Corvette-Type Warship. *KAPAL*. 12(3): 158–164. https://doi.org/10.14710/kpl.v12i3.9979

Rahmaji T, Prabowo AR, Tuswan T, Muttaqie T, Muhayat N, Baek SJ. 2022. Design of Fast Patrol Boat for Improving Resistance, Stability, and Seakeeping Performance. *Designs*. 6(6): 1–48. https://doi.org/10.3390/designs6060105

Romadhoni. 2016. Maneuvering Analysis of an Axe Bow-Type Vessel in Regular Waves. *KAPAL*. 13(2): 61–68. https://doi.org/10.14710/kpl.v13i2.11488

Romadhoni. 2019. *A*nalisa Seakeeping Ferformance Kapal Cepat Model Planing Hull Chine. *Inovtek Polbeng: Jurnal Inovasi Teknologi Politeknik Negeri Bengkalis*. 9(1): 30–37. https://doi.org/10.35314/ip.v9i1.887

Saifullah NN, Prabowo AR, Muhayat N, Tuswan T, Harsito C, Adiputra R, Jurkovič M, Baek, SJ. 2024. Leisure Boat Design: A Comprehensive Study of the Shape and Dimension Effects on Hydrodynamic Performances. *Evergreen.* 11*(3):* 2091-2199. *https://doi.org/10.5109/7236854*.

Suzuki R, Tsukada Y, Ueno M. 2023. Effects of Steady Wave Forces on Course-Keeping Manoeuvres of Full and Model-Scale Ships Moving Obliquely in Short Waves. *Ship Technology Research*. 70(3): 190–208. https://doi.org/10.1080/09377255.2022.2149094

Virliani P, Suastika IK, Aryawan WD. 2017. Numerical Analysis of Submarine Maneuvering with Variations in Afterbody Shape. *Jurnal Kelautan Nasional*. 12(2): 73–81. https://doi.org/10.15578/jkn.v12i2.5703